

# Peripapillary Atrophy Area as an Indicator of Glaucomatous Structural and Functional Progression

Maroun Khreish<sup>1</sup>, Joel S. Schuman<sup>1-5</sup>, TingFang Lee<sup>1,6</sup>, Zeinab Ghassabi<sup>1</sup>, Ronald Zambrano<sup>1</sup>, Jiyuan Hu<sup>6</sup>, Hiroshi Ishikawa<sup>7</sup>, Gadi Wollstein<sup>1,2,5</sup>, and Fabio Lavinsky<sup>8</sup>

<sup>1</sup> Department of Ophthalmology, NYU Langone Health, New York, NY, USA

<sup>2</sup> Department of Biomedical Engineering, NYU Tandon School of Engineering, Brooklyn, NY, USA

<sup>3</sup> Department of Electrical and Computer Engineering, NYU Tandon School of Engineering, Brooklyn, NY, USA

<sup>4</sup> Department of Neuroscience and Physiology, NYU Langone Health, New York, NY, USA

<sup>5</sup> Center for Neural Science, NYU College of Arts and Sciences, New York, NY, USA

<sup>6</sup> Department of Population Health, NYU Langone Health, New York, NY, USA

<sup>7</sup> Department of Ophthalmology, Medical Informatics and Clinical Epidemiology, Oregon Health & Science University, Portland, OR, USA

<sup>8</sup> Universidade do Vale do Rio dos Sinos Medical School, Sao Leopoldo, Brazil

**Correspondence:** Gadi Wollstein, Wills Eye Hospital, 840 Walnut Street, Philadelphia, PA 19107, USA. e-mail: [gwillstein@willseye.org](mailto:gwillstein@willseye.org)

**Received:** June 2, 2023

**Accepted:** January 16, 2024

**Published:** March 1, 2024

**Keywords:** peripapillary atrophy; optical coherence tomography; glaucoma; progression

**Citation:** Khreish M, Schuman JS, Lee T, Ghassabi Z, Zambrano R, Hu J, Ishikawa H, Wollstein G, Lavinsky F. Peripapillary atrophy area as an indicator of glaucomatous structural and functional progression. *Transl Vis Sci Technol.* 2024;13(3):1, <https://doi.org/10.1167/tvst.13.3.1>

**Purpose:** To determine whether peripapillary atrophy (PPA) area is an indicator of glaucomatous structural and functional damage and progression.

**Methods:** In this retrospective longitudinal analysis from ongoing prospective study we qualified 71 eyes (50 subjects) with glaucoma. All subjects had a comprehensive ophthalmic examination, visual field (VF), and spectral-domain optical coherence tomography (OCT) testing in at least three visits. PPA was manually delineated on en face OCT optic nerve head scans, while observing the corresponding cross-sectional images, as the hyper-reflective area contiguous with the optic disc.

**Results:** The mean follow-up duration was  $4.4 \pm 1.4$  years with an average of  $6.8 \pm 2.2$  visits. At baseline, PPA area was significantly associated only with VF's mean deviation (MD;  $P = 0.041$ ), visual field index (VFI;  $P = 0.041$ ), superior ganglion cell inner plexiform layer (GCIPL;  $P = 0.011$ ), and disc area ( $P = 0.011$ ). Longitudinally, PPA area was negatively and significantly associated with MD ( $P = 0.015$ ), VFI ( $P = 0.035$ ), GCIPL ( $P = 0.009$ ), superior GCIPL ( $P = 0.034$ ), and disc area ( $P = 0.007$ , positive association).

**Conclusions:** Longitudinal change in PPA area is an indicator of glaucomatous structural and functional progression but PPA area at baseline cannot predict future progression.

**Translational Relevance:** Longitudinal changes in peripapillary atrophy area measured by OCT can be an indicator of structural and functional glaucoma progression.

## Introduction

Glaucoma is an optic neuropathy that damages the optic nerve structurally and functionally.<sup>1,2</sup> It is the leading cause of irreversible vision loss and the second leading cause of overall vision loss worldwide.<sup>3,4</sup> There is large variability in glaucoma presentation and progression between individuals. The slow but irreversible nature of glaucoma progression makes early and reliable detection critical for management

and preservation of functional vision. Indicators of a worse clinical course and a faster progression rate might assist in achieving this goal. Studies have identified prognostic factors for future glaucoma progression including age, intraocular pressure (IOP), IOP fluctuation, retinal nerve fiber layer (RNFL) thickness, and ganglion cell inner plexiform layer (GCIPL) thickness.<sup>5,6</sup> It has been suggested that there are different phenotypes and patterns of glaucomatous optic disc injury, and each phenotype is associated with several distinctive clinical features.<sup>7,8</sup>

Peripapillary atrophy (PPA) is a morphological feature located adjacent to the optic nerve margin that is divided into zones. The  $\beta$  zone PPA is defined as a crescent of chorioretinal atrophy directly adjacent to the optic disc margin, characterized by visible sclera and choroidal vessels.<sup>9,10</sup> Most existing research investigating the role of PPA in glaucoma has relied on stereophotography evaluations. This includes a prior study that demonstrated that the  $\beta$  zone PPA is more prevalent and larger in glaucomatous eyes than in healthy eyes.<sup>11</sup> Other studies have reported an association between the presence of  $\beta$  zone PPA and an increased risk for visual field (VF) progression.<sup>12,13</sup> It was also reported that the region of largest  $\beta$  zone PPA is associated with the hemifield of fastest VF progression.<sup>14</sup> However, no significant association has been found between longitudinal  $\beta$  zone PPA progression and faster VF progression.<sup>13</sup> A recent study with 10 years follow-up used disc photography and optical coherence tomography (OCT)–generated RNFL thickness measurements reported that PPA enlargement was significantly more common in subjects with RNFL defect progression than in eyes without progression.<sup>15</sup>

The introduction of OCT into routine glaucoma management provides the opportunity to leverage its micron-scale resolution and highly reproducible measurements for precise PPA quantification. Previous cross-sectional OCT studies have shown significant differences between healthy and glaucomatous eyes when PPA was evaluated quantitatively in OCT images.<sup>16,17</sup> In the current study, we will use OCT to precisely quantify the PPA and determine its longitudinal association with structural and functional changes in glaucoma. We also examine the capability of baseline PPA measurements to predict glaucoma progression. This information will establish the role of a widely used clinical tool, such as OCT, in quantitatively and longitudinally evaluating PPA area as a valuable biomarker for glaucoma progression.

## Methods

Subjects with glaucoma were enrolled from our ongoing prospective, longitudinal study designed to assess ocular structure over time. The institutional review boards and ethics committees at New York University and the University of Pittsburgh approved the study. The study followed the tenets of the Declaration of Helsinki and was conducted in compliance with the Health Insurance Portability and Accountability Act. Informed consent was obtained from all subjects.

## Participants

Subjects with open-angle glaucoma were recruited to this study if they were 40 years old or older, had no history of diabetes or any systemic disease or medication usage that might affect the visual system, and no major ocular trauma or ocular surgeries other than uncomplicated cataract or glaucoma surgeries performed before enrollment. Subjects had best-corrected visual acuity of 20/60 or better, spherical equivalent within 4D to  $-8D$ , axial length (AL)  $<28$  mm, no media opacity precluding reliable VF testing or OCT scanning and no intraocular comorbidity other than glaucoma. All subjects had at least three visits, each of them at least four months apart, unless otherwise medically indicated. Glaucoma diagnosis required at least two consecutive reliable VFs with glaucoma hemifield tests outside normal limits or a cluster of three or more non-edge points in a location typical for glaucoma, with all points depressed on the pattern deviation plot at the  $p < 5\%$  level and at least one point depressed at the  $p < 1\%$  level.

## Study Protocol

All subjects underwent a full ocular examination including refraction, best-corrected visual acuity, biomicroscopy, gonioscopy, Goldman applanation tonometry and fundus examination. AL was measured with Lenstar (Haag-Streit, Mason, OH, USA). VF was tested with Swedish interactive thresholding algorithm (SITA standard; Humphrey Field Analyzer; Zeiss, Dublin, CA, USA) 24-2 perimetry. A VF test was considered reliable if it had less than 33% false-positive or false-negative responses and fixation losses. Mean deviation (MD) and visual field index (VFI) were used for the analysis. All subjects were imaged with SD-OCT (Cirrus HD-OCT; Zeiss) using the Macular Cube 200  $\times$  200 and the Optic Disc Cube 200  $\times$  200 scans. Scans were disqualified if they had a signal strength  $<7$ , decentration of the RNFL sampling circle, segmentation errors or motion artifacts defined as a discontinuity of the blood vessels that exceeded the width of one major vessel diameter. Peripapillary RNFL (global and quadrants), macular GCIPL (global and sectorial) thicknesses, disc area, rim area, MD, and VFI were used for the analysis.

PPA was manually delineated on the en face ONH scan while observing the relevant b-scans using acceptable landmarks: Bruch's membrane opening for optic disc margins and retinal pigment epithelium atrophy for PPA margins. PPA area was delineated as the area contiguous with the optic disc with the presence of hyper- or hyporeflectivity using a software of our

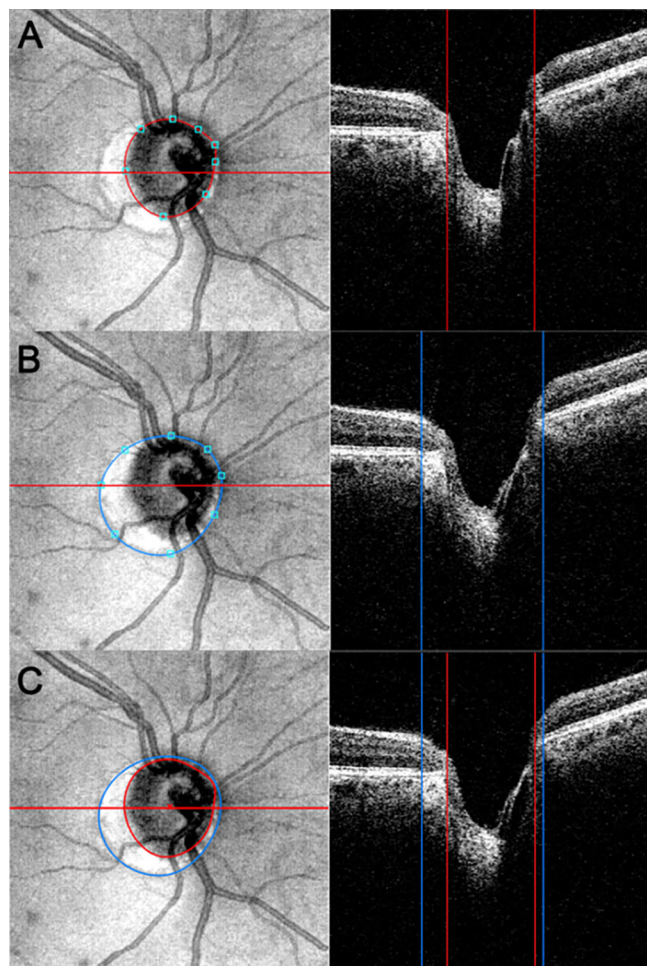


**Figure 1.** Method of measuring PPA area on OCT scans. (A) Disc margin was manually delineated (red circle) on the en face image while observing corresponding B-scan. (B) Similarly, the distal PPA margin was marked (blue line). (C) The area contained between the two circles is measured as the PPA area.

own design. Two margins were manually drawn: at the optic disc margin and at the PPA margin (Fig. 1). The crescent-shaped area between these two lines was measured as total and quadrant PPA areas. Quadrant PPA measurements were oriented similar to quadrant RNFL measurements provided by Cirrus OCT, but for GC IPL the device provides 60° sectoral measurement that was used for the analysis.

To determine the reproducibility of our PPA area delineation, a subset of 35 eyes (35 subjects) was randomly selected. Each eye chosen in this subset was measured twice by the same examiner.

Guided progression analysis (GPA) is a method provided by the OCT and VF devices to determine progression. The proportion of eyes showing a significant rate of progression (trend-based progression) for RNFL, GC IPL, and MD was recorded. The

OCT's GPA also reports change from baseline for these parameters that significantly exceed expected population-derived change as progression (event-based progression). If significant changes are detected in the same location in 2 consecutive tests, the eye is labeled by the software as "possible progression." Changes that persist in three consecutive tests are labeled as "likely progression." Both "possible" and "likely" were considered as progressing for the analysis. For the subanalysis of progression defined by GPA, we included only eyes with at least four qualified OCTs and VFs, which is the minimal number of tests required by the software.

## Statistical Analysis

Continuous variables that follow a normal distribution are expressed as mean  $\pm$  standard deviation (SD), and variables with a skewed distribution are expressed as mean (interquartile range). Measurement reproducibility was determined using within subject coefficient of variations. Linear mixed-effects models were used to evaluate (1) the association between PPA area and OCT and VF parameters at baseline while adjusting for age, central corneal thickness, gender, and AL; (2) the longitudinal association between PPA area and OCT and VF parameters while adjusting for age at baseline and AL and accounting for repeated measurements over time; (3) the association between baseline PPA area and the rate of change in VF and OCT parameters while adjusting for age at baseline and AL; and (4) the difference in baseline PPA area between GPA-defined progressors or non-progressors eyes. Intereye correlation was accounted for in all models. The rate of change in VF and OCT parameters was estimated by linear regression model. The *p* value of each association was obtained via Satterthwaite's degrees of freedom method. Additionally, the Benjamini-Hochberg procedure was applied to the association analyses to account for the multiple comparisons and reported as an adjusted *P* value. A *P* value  $<0.05$  was considered statistically significant. R language and environment for statistical computing program (version 3.3.2) was used for statistical analysis.<sup>18</sup> The linear mixed-effect models were performed through the lme4<sup>19</sup> and lmerTest<sup>20</sup> R packages.

## Results

Seventy-one eyes from 50 subjects were qualified for the study. Twenty-eight subjects were female (56%), and the ethnicity profile was as follows: 36 White (72%), 13 African-American (26%) and 1 Asian (2%). The mean



**Table 1.** Baseline VF and OCT Measurements of the Study Population (71 Eyes)

Parameter	Mean (SD)
Age (years)	58.7 ± 10.3
Follow-up duration (years)	4.4 ± 1.4
Number of visits	6.8 ± 2.2
AL (mm)	24.2 ± 1.3
CCT (μm)	558 ± 49.8
MD (dB)*	−1.98 (−6.97, −0.73)
VFI (%)*	97 (83.5, 98)
Average RNFL (μm)	72.14 ± 12.28
Superior RNFL (μm)	85.41 ± 18.19
Inferior RNFL (μm)	86.24 ± 24.14
Average GCIPL (μm)	68.06 ± 9.22
Superior GCIPL (μm)	69.06 ± 9.95
Inferior GCIPL (μm)	66.59 ± 9.86
Disc Area (mm <sup>2</sup> )	1.79 ± 0.48
Rim Area (mm <sup>2</sup> )	0.87 ± 0.23
PPA area (mm <sup>2</sup> )	2.55 ± 0.75
Superior PPA area (mm <sup>2</sup> )	0.54 ± 0.21
Inferior PPA area (mm <sup>2</sup> )	0.67 ± 0.26

CCT, central corneal thickness.

\*Median (25%, 75% quartiles).

follow-up duration was 4.4 ± 1.4 years with an average of 6.8 ± 2.2 number of visits. The baseline characteristics are summarized in [Table 1](#).

### Measurement Reproducibility

The within subject coefficient of variations of disc area and PPA area were 0.017 (95%CI: 0.013–0.021)

and 0.019 (95%CI: 0.015–0.025), respectively, reflecting an excellent reproducibility.

### Baseline PPA Measurements and OCT and VF Parameters

Association between baseline PPA area and functional parameters measured with the visual field (VFI and MD), and OCT structural parameters (average RNFL, average GCIPL and their corresponding sectoral measurements) was performed using 71 eyes ([Table 2](#); [Fig. 2](#)). Significant negative associations were detected between baseline PPA area and MD, VFI, and superior GCIPL. A marginally significant association was detected between PPA area and average GCIPL. A significant positive association was detected between baseline PPA area and disc area. No significant association was detected between other sectoral PPA area and corresponding structural measurements. Age, central corneal thickness, gender and AL were not significant in any of the models.

### Longitudinal change in PPA Measurements and OCT and VF Parameters

In the longitudinal analysis of PPA area, we evaluated 484 scans of 71 eyes acquired during the follow-up period. The PPA area significantly increased over time while all other VF and OCT parameters (with the expected exception of disc area) decreased significantly over time ([Table 3](#)). When we evaluated the association between longitudinal PPA and VF and OCT parameters, we observed significant negative association

**Table 2.** Association Between PPA Area Measurements at Baseline With VF and OCT Parameters at Baseline While Accounting for Gender, Age, CCT, and AL (71 Eyes)

Parameter	Coefficient (95% CI)	Nominal <i>P</i> Value	Adjusted <i>P</i> Value
MD (dB)	− <b>0.031 (−0.057, −0.004)*</b>	<b>0.027*</b>	<b>0.041*</b>
VFI (%)	− <b>0.010 (−0.019, −0.001)*</b>	<b>0.041*</b>	<b>0.041*</b>
Average RNFL (μm)	−0.010 (−0.023, 0.003)	0.123	0.246
Superior RNFL (μm) <sup>†</sup>	−0.002 (−0.004, 0.001)	0.246	0.393
Inferior RNFL (μm) <sup>†</sup>	−0.001 (−0.003, 0.002)	0.541	0.541
Average GCIPL (μm)	−0.016 (−0.032, 0.001)	0.061	0.163
Superior GCIPL (μm) <sup>†</sup>	− <b>0.007 (−0.011, −0.003)*</b>	<b>0.003*</b>	<b>0.011*</b>
Inferior GCIPL (μm) <sup>†</sup>	−0.002 (−0.008, 0.003)	0.397	0.529
Disc Area (mm <sup>2</sup> )	<b>0.721 (0.294, 1.148)*</b>	<b>0.002*</b>	<b>0.011*</b>
Rim Area (mm <sup>2</sup> )	−0.282 (−1.084, 0.520)	0.494	0.541

CCT, central corneal thickness.

\*Values in bold font are statistically significant.

<sup>†</sup>Association with corresponding sectoral PPA Area.

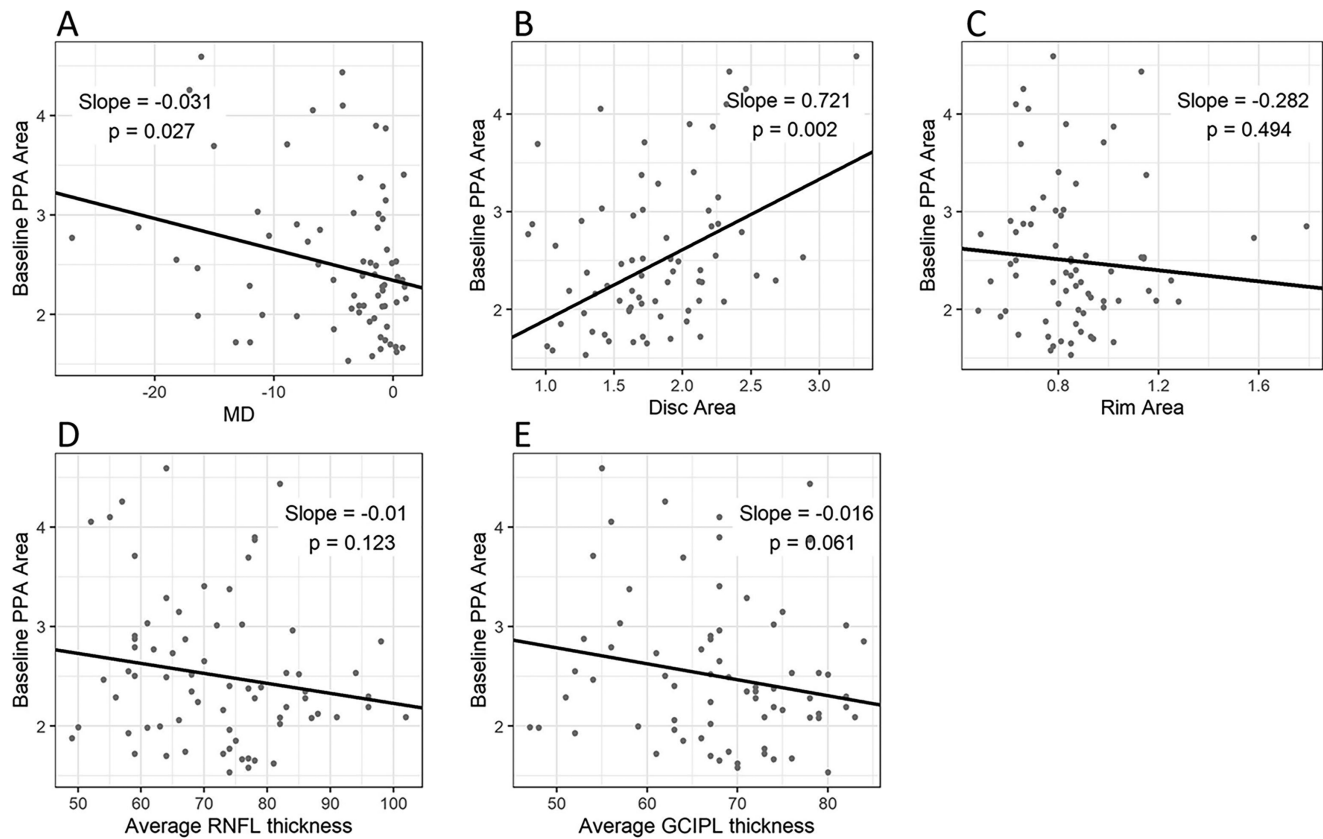


**Figure 2.** Scatter plots between baseline PPA area measurements and VF and OCT parameters at baseline: (A) MD, (B) Disc area, (C) Rim area, (D) Average RNFL thickness, and (E) Average GCIPL thickness.

**Table 3.** Rate of Change of PPA Area, VF, and OCT Parameters Per Year (71 Eyes)

Parameter	Estimated Rate of Change/Year (95% CI)	Nominal P Value*	Adjusted P Value
MD (dB/yr)	<b>−0.183 (−0.255, −0.110)<sup>†</sup></b>	<b>&lt;0.001<sup>†</sup></b>	<b>&lt;0.001<sup>†</sup></b>
VFI (%/yr)	<b>−0.401 (−0.616, −0.186)<sup>†</sup></b>	<b>&lt;0.001<sup>†</sup></b>	<b>&lt;0.001<sup>†</sup></b>
Average RNFL (μm/yr)	<b>−0.396 (−0.544, −0.247)<sup>†</sup></b>	<b>&lt;0.001<sup>†</sup></b>	<b>&lt;0.001<sup>†</sup></b>
Superior RNFL (μm) <sup>‡</sup>	<b>−0.738 (−0.967, −0.509)<sup>†</sup></b>	<b>&lt;0.001<sup>†</sup></b>	<b>&lt;0.001<sup>†</sup></b>
Inferior RNFL (μm) <sup>‡</sup>	<b>−0.749 (−0.974, −0.525)<sup>†</sup></b>	<b>&lt;0.001<sup>†</sup></b>	<b>&lt;0.001<sup>†</sup></b>
Average GCIPL (μm/yr)	<b>−0.362 (−0.439, −0.284)<sup>†</sup></b>	<b>&lt;0.001<sup>†</sup></b>	<b>&lt;0.001<sup>†</sup></b>
Superior GCIPL (μm) <sup>‡</sup>	<b>−0.353 (−0.464, −0.241)<sup>†</sup></b>	<b>&lt;0.001<sup>†</sup></b>	<b>&lt;0.001<sup>†</sup></b>
Inferior GCIPL (μm) <sup>‡</sup>	<b>−0.448 (−0.532, −0.363)<sup>†</sup></b>	<b>&lt;0.001<sup>†</sup></b>	<b>&lt;0.001<sup>†</sup></b>
Disc Area (mm <sup>2</sup> /yr)	−0.002 (−0.006, 0.001)	0.135	0.135
Rim Area (mm <sup>2</sup> /yr)	<b>−0.008 (−0.010, −0.006)<sup>†</sup></b>	<b>&lt;0.001<sup>†</sup></b>	<b>&lt;0.001<sup>†</sup></b>
PPA area (mm <sup>2</sup> /yr)	<b>0.053 (0.038, 0.069)<sup>†</sup></b>	<b>&lt;0.001<sup>†</sup></b>	<b>&lt;0.001<sup>†</sup></b>
Superior PPA area (mm <sup>2</sup> /yr)	<b>0.011 (0.005, 0.016)<sup>†</sup></b>	<b>&lt;0.001<sup>†</sup></b>	<b>&lt;0.001<sup>†</sup></b>
Inferior PPA area (mm <sup>2</sup> /yr)	<b>0.017 (0.010, 0.024)<sup>†</sup></b>	<b>&lt;0.001<sup>†</sup></b>	<b>&lt;0.001<sup>†</sup></b>

\* P values for comparison with a zero slope.  
<sup>†</sup> Values in bold font are statistically significant.  
<sup>‡</sup> Association with corresponding sectoral PPA Area.

**Table 4.** Association Between Longitudinal PPA Area Measurements With VF and OCT Parameters Measured Longitudinally (71 Eyes)

Parameter	Coefficients (95% CI)	Nominal <i>P</i> Value	Adjusted <i>P</i> Values
MD (dB)	<b>−0.022 (−0.039, −0.006)*</b>	<b>0.007*</b>	<b>0.015*</b>
VFI (%)	<b>−0.006 (−0.012, −0.001)*</b>	<b>0.035*</b>	<b>0.035*</b>
Average RNFL (μm)	−0.006 (−0.014, 0.002)	0.132	0.177
Superior RNFL (μm) <sup>†</sup>	0.000 (−0.002, 0.002)	0.991	0.991
Inferior RNFL (μm) <sup>†</sup>	−0.002 (−0.003, 0.001)	0.112	0.177
Average GCIPL (μm)	<b>−0.020 (−0.032, −0.007)*</b>	<b>0.002*</b>	<b>0.009*</b>
Superior GCIPL (μm) <sup>†</sup>	<b>−0.004 (−0.007, −0.001)*</b>	<b>0.013*</b>	<b>0.034*</b>
Inferior GCIPL (μm) <sup>†</sup>	−0.004 (−0.008, 0.001)	0.109	0.177
Disc Area (mm <sup>2</sup> )	<b>0.559 (0.238, 0.881)*</b>	<b>0.001*</b>	<b>0.007*</b>
Rim Area (mm <sup>2</sup> )	−0.209 (−0.679, 0.261)	0.384	0.438

\*Values in bold font are statistically significant.

<sup>†</sup>Association with corresponding sectoral PPA area.

**Table 5.** Association Between Baseline PPA Area Measurements and the Rate of Change of VF and OCT Parameters (71 Eyes)

Parameter	Coefficient (95% CI)	Nominal <i>P</i> Value	Adjusted <i>P</i> Values
MD (db/year)	−0.036 (−0.173, 0.101)	0.610	0.610
VFI (%/year)	−0.133 (−0.545, 0.279)	0.531	0.610
Average RNFL (μm/yr)	0.139 (−0.222, 0.500)	0.454	0.664
Superior RNFL (μm/yr) <sup>†</sup>	0.029 (−1.834, 1.892)	0.976	0.976
Inferior RNFL (μm/yr) <sup>†</sup>	<b>1.638 (0.054, 3.222)*</b>	<b>0.047*</b>	<b>0.187*</b>
Average GCIPL (μm/yr)	0.131 (−0.051, 0.312)	0.163	0.435
Superior GCIPL (μm/yr) <sup>†</sup>	0.133 (−0.779, 1.045)	0.776	0.887
Inferior GCIPL (μm/yr) <sup>†</sup>	<b>0.686 (0.104, 1.268)*</b>	<b>0.024*</b>	<b>0.187*</b>
Disc Area (mm <sup>2</sup> /yr)	−0.003 (−0.010, 0.004)	0.381	0.664
Rim Area (mm <sup>2</sup> /yr)	−0.002 (−0.007, 0.003)	0.498	0.664

\*Values in bold font are statistically significant.

<sup>†</sup>Association with corresponding sectoral PPA area.

with VF parameters and similarly only for global and superior GCIPL (Table 4). A significant positive association was detected with disc area. Associations with age and AL were not significant in the models.

### PPA Area at Baseline and Rate of Change of VF and OCT Parameters

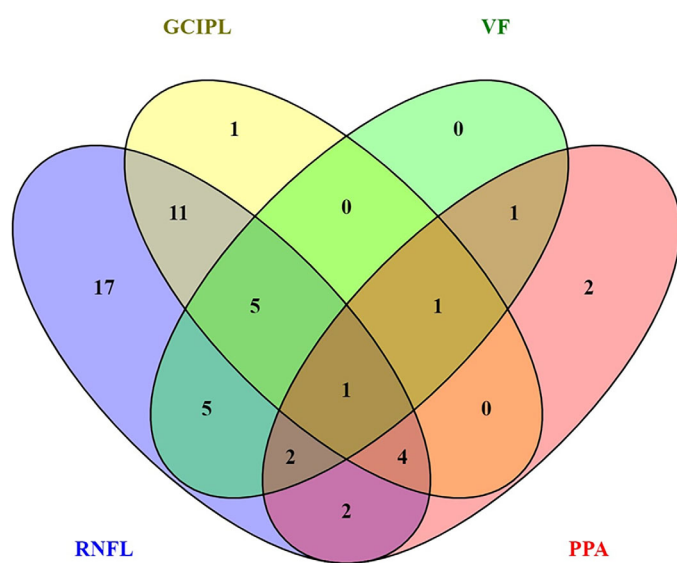
No significant association was detected between baseline PPA area and the rates of change of global and sectoral parameters, based on the adjusted *P* values (Table 5). Associations with age and AL were not significant in the models.

### Difference at Baseline PPA Area Between VF and OCT GPA Progressors and Nonprogressors

Sixty-one eyes qualified for the GPA analysis. No significant difference was detected when comparing the baseline demographic characteristics between the original 71 eyes and the GPA subset. Among these 61 eyes, 15 eyes progressed according to VF GPA report. Using OCT GPA analysis, 47 eyes progressed according to RNFL report and 23 eyes progressed according to GCIPL report. When baseline PPA area was compared between VF and OCT GPA progressors and nonprogressors, no significant difference was

**Table 6.** Differences of Baseline PPA Area Measurements Between GPA's Progressors and Nonprogressors (61 Eyes)

Parameter	Progressors	Differences		
		Estimates	SE	P Value
RNFL progressors vs. nonprogressors	47 (77%)	0.291	0.209	0.172
GCIPL progressors vs. nonprogressors	23 (38%)	0.288	0.185	0.127
VF progressors vs. nonprogressors	15 (25%)	−0.066	0.225	0.770

**Figure 3.** Venn diagram of the number of eyes progressing by PPA area, and the GPA analysis of VF, OCT RNFL, and GCIPL.

detected for any tested parameter (Table 6). A summary of all GPA progressing eyes and eyes where the PPA area rate of change was significantly different than a zero-slope demonstrated that although the absolute number of eyes defined as progressors by PPA area was relatively low, most of them (11/13) showed progression with at least one other method (Fig. 3).

## Discussion

Our study evaluated the ability of PPA area, measured with OCT, as an indicator of structural and functional progression in glaucoma. We determined that at baseline the PPA area was significantly associated only with MD, VFI, and superior GCIPL, but when assessed longitudinally it was associated with the longitudinal change in measurements of functional parameters (MD, VFI) and structural parameters (GCIPL globally and in the superior quadrant). This study is the first to quantitatively demonstrate that

longitudinal changes in PPA indicate glaucomatous structural and functional progression.

We did not identify any significant association cross-sectionally at baseline between PPA area and any of the tested parameters except for negative association with MD, VFI, and superior GCIPL (a more negative MD, VFI, and superior GCIPL are associated with larger PPA area and vice versa) (Table 2). The positive association with disc area is expected because it is common for myopic eyes to have a large disc and PPA.<sup>21,22</sup> We can therefore conclude that PPA is a reliable indicator for the presence of functional glaucomatous damage and for structural damage in the superior macula. This finding contradicts previous studies that reported a significant association between an increase in PPA area and OCT optic nerve head parameters (decreased rim area, and increased vertical cup to disc ratio and cup area).<sup>23</sup> However, the participants in the previous study had larger optic discs, smaller PPA and substantially more severe glaucoma (mean VF MD:  $-9.69 \pm 8.44$  dB) than our cohort, which might explain this discrepancy.

Despite the minimal cross-sectional association between PPA area and structural measurements in our study, there was a significant association longitudinally with both structure and function (Table 4). This finding is in agreement with Uchida et al.<sup>24</sup> who evaluated PPA area progression qualitatively, by three observers who evaluated standard color stereoscopic fundus photographs. Similar to our study, they reported that progression of PPA was associated with progressive optic disc damage and progressive VF loss. In contrast, De Moraes et al.<sup>13</sup> also analyzed stereophotographs and reported that PPA area progression is not associated with faster visual field progression. The discrepancy with the later study might be explained by the qualitative method that was used to assess new appearance or change in PPA area in stereophotographs at baseline and at the end of follow-up, whereas our study measured PPA area quantitatively.

In our study, PPA area was negatively and significantly associated with both MD and VFI and among the structural parameters was negatively and significantly associated with average and superior GCIPL

thickness. The latter association was significant even though the sectoral GCIPL measurements included sectors of only 60°. To verify that this finding is not due to unbalanced prevalence of the location of the VF defect, we evaluated the location of baseline VF damage but could not find a clear propensity to either one of the hemifields. The reason for the disparity between the superior and inferior sectors is therefore unclear. Our findings corroborate a previous study in which PPA area was determined using stereophotography and showed that the location of largest  $\beta$  zone PPA can predict the location of most rapid VF progression.<sup>14</sup>

We also reported a strong and positive association between rate of change of PPA and change in disc area (Table 4), even though disc area was the only parameter that did not show any change over time, as expected (Table 3). The explanation for this seemingly contradictory result is that although larger discs do not significantly change over time, they are associated with faster progression of PPA area, and vice versa.

As part of our longitudinal analysis, we also examined progression using GPA criteria (Fig. 3). It is noticeable that there is marked overlap between eyes defined as PPA area progression and those that progressed by other criteria. Only two eyes were solely determined as progressors by PPA and we could not identify any unique characteristics for this small subgroup. We can therefore conclude that enlargement of PPA area over time is an indicator of glaucoma worsening.

Finally, we evaluated the ability of baseline PPA area measurements to predict future structural and functional rate of change (Table 5). Only inferior PPA area was significantly associated with inferior RNFL and inferior GCIPL future rate of progression; however, when  $P$  value were adjusted for multiple comparisons, there was no significant association (Table 5). Despite the fact that this association is not statistically significant, it shows that inferior PPA at baseline is the best predictor of the future progression of inferior RNFL and inferior GCIPL. Our findings corroborate with those reported in a previous study where glaucoma eyes were divided into two groups according to the presence or absence of  $\beta$ -zone PPA in stereophotographs.<sup>25</sup> Eyes with  $\beta$ -zone PPA showed a significantly faster rate of RNFL thinning in OCT scans than did eyes without  $\beta$ -zone PPA in the inferior quadrant and 7 o'clock sector. These findings align with previous studies that have identified the inferior macula as a region highly susceptible to early glaucomatous damage.<sup>26,27</sup> Although the reasons for increased susceptibility in this particular location remain unclear, our findings add to the

growing body of evidence in support of this notion. Additionally, we assessed the predictive capability of PPA area by comparing baseline measurements in groups categorized as progressors and nonprogressors using GPA but did not find any significant difference.

Because PPA is also common in myopic eyes and progresses longitudinally in myopic patients,<sup>28–30</sup> we limited our cohort to subjects with AL < 28 mm. Furthermore, we included AL as a covariable in all models. However, AL was not statistically significant in any of our models and thus did not play a role in our population which only included a small number of eyes had within the range of 26–28 mm (10 eyes). Therefore our results might not apply to high myopic eyes with glaucoma exhibiting PPA.

The delineation of PPA area was performed manually, which might lead to increased measurement variability. Currently there is no fully automated method to delineate this region. We made all efforts to carefully perform this task by marking its boundaries on the enface images while consulting the cross-sectional images to improve certainty of the selected location. Furthermore, the high reproducibility we reported supports the reliability of our delineation. Using our method, we were unable to measure the PPA area reliably when divided into zones (alpha, beta, gamma). Based on our results, a future study when dividing the PPA area into zones is warranted. Another potential limitation of the study is that sectoral GCIPL measurements included sectors of only 60°, whereas sectoral RNFL measurements are of 90°. This is an inevitable limitation because the size of these sectors is defined by the native operating software of the device. Nevertheless, we demonstrated significant association between superior PPA area and superior GCIPL along with global associations. Finally, our study did not include healthy individuals, and future prospective studies comparing longitudinal changes in healthy and glaucomatous eyes with PPA are warranted. In conclusion, longitudinal change in PPA area over time can be an indicator for structural and functional progression in subjects with glaucoma.

## Acknowledgments

Supported by NIH R01-EY013178, P30-EY013079, an unrestricted grant from Research to Prevent Blindness.

Disclosure: M. Khreish, None; J.S. Schuman, receives royalties for intellectual property licensed



by Massachusetts Institute of Technology and Massachusetts Eye and Ear Infirmary to Zeiss; T. Lee, None; Z. Ghassabi, None; R. Zambrano, None; J. Hu, None; H. Ishikawa, None; G. Wollstein, None; F. Lavinsky, None

## References

1. Flaxman SR, Bourne RRA, Resnikoff S, et al. Global causes of blindness and distance vision impairment 1990–2020: a systematic review and meta-analysis. *Lancet Glob Health*. 2017;5(12):e1221–e1234.
2. Weber AJ, Harman CD, Viswanathan S. Effects of optic nerve injury, glaucoma, and neuroprotection on the survival, structure, and function of ganglion cells in the mammalian retina. *J Physiol*. 2008;586:4393–4400.
3. Kingman S. Glaucoma is second leading cause of blindness globally. *Bull World Health Organ*. 2004;82:887–888.
4. Quigley HA, Broman AT. The number of people with glaucoma worldwide in 2010 and 2020. *Br J Ophthalmol*. 2006;90:262–267.
5. Ernest PJ, Schouten JS, Beckers HJ, et al. An evidence-based review of prognostic factors for glaucomatous visual field progression. *Ophthalmology*. 2013;120:512–519.
6. Zhang X, Dastiridou A, Francis BA, et al. Baseline Fourier-domain optical coherence tomography structural risk factors for visual field progression in the Advanced Imaging for Glaucoma Study. *Am J Ophthalmol*. 2016;172:94–103.
7. Nicolela MT, Drance SM. Various glaucomatous optic nerve appearances: clinical correlations. *Ophthalmology*. 1996;103:640–649.
8. Broadway DC, Nicolela MT, Drance SM. Optic disk appearances in primary open-angle glaucoma. *Surv Ophthalmol*. 1999;43(Suppl 1):S223–S243.
9. Jonas JB, Nguyen XN, Gusek GC, et al. Parapapillary chorioretinal atrophy in normal and glaucoma eyes. I. Morphometric data. *Invest Ophthalmol Vis Sci*. 1989;30:908–918.
10. Jonas JB, Fernández MC, Naumann GO. Glaucomatous parapapillary atrophy. Occurrence and correlations. *Arch Ophthalmol*. 1992;110:214–222.
11. Jonas JB, Naumann GO. Parapapillary chorioretinal atrophy in normal and glaucoma eyes. II. Correlations. *Invest Ophthalmol Vis Sci*. 1989;30:919–926.
12. Teng CC, De Moraes CG, Prata TS, et al. Beta-Zone parapapillary atrophy and the velocity of glaucoma progression. *Ophthalmology*. 2010;117:909–915.
13. De Moraes CG, Murphy JT, Kaplan CM, et al.  $\beta$ -Zone Parapapillary Atrophy and Rates of Glaucomatous Visual Field Progression: african descent and glaucoma evaluation study. *JAMA Ophthalmol*. 2017;135(6):617–623.
14. Teng CC, De Moraes CG, Prata TS, et al. The region of largest  $\beta$ -zone parapapillary atrophy area predicts the location of most rapid visual field progression. *Ophthalmology*. 2011;118:2409–2413.
15. Bak E, Kim YW, Kim YK, et al. Ten-year-and-beyond longitudinal change of  $\beta$ -zone parapapillary atrophy in glaucoma: association with retinal nerve fibre layer defect. *Br J Ophthalmol*. 2022;106:1393–1398.
16. Manjunath V, Shah H, Fujimoto JG, et al. Analysis of peripapillary atrophy using spectral domain optical coherence tomography. *Ophthalmology*. 2011;118:531–536.
17. Manalastas PIC, Belghith A, Weinreb RN, et al. Automated beta zone parapapillary area measurement to differentiate between healthy and glaucoma eyes. *Am J Ophthalmol*. 2018;191:140–148.
18. R Core Team. *R: a language and environment for statistical computing*. 2022.
19. Bates D, Mächler M, Bolker B, et al. Fitting linear mixed-effects models using lme4. *J Stat Software*. 2015;67(1):1–48.
20. Kuznetsova A, Brockhoff PB, Christensen RHB. lmerTest Package: tests in linear mixed effects models. *J Stat Software*. 2017;82(13):1–26.
21. Moon Y, Lim HT. Relationship between peripapillary atrophy and myopia progression in the eyes of young school children. *Eye (Lond)*. 2021;35:665–671.
22. Jabbarpoor Bonyadi MH. High myopic peripapillary atrophy; spectral domain optical coherence tomography features. *J Ophthalmic Vis Res*. 2016;11:124–125.
23. Uhm KB, Lee DY, Kim JT, et al. Peripapillary atrophy in normal and primary open-angle glaucoma. *Korean J Ophthalmol*. 1998;12(1):37–50.
24. Uchida H, Ugurlu S, Caprioli J. Increasing peripapillary atrophy is associated with progressive glaucoma. *Ophthalmology*. 1998;105(8):1541–1545.
25. Lee EJ, Kim T-W, Weinreb RN, et al.  $\beta$ -zone parapapillary atrophy and the rate of retinal nerve fiber layer thinning in glaucoma. *Invest Ophthalmol Vis Sci*. 2011;52:4422–4427.
26. Hood DC. Improving our understanding, and detection, of glaucomatous damage: an approach

- based upon optical coherence tomography (OCT). *Prog Retin Eye Res.* 2017;57:46–75.
27. Hood DC, Raza AS, de Moraes CG, et al. Glaucomatous damage of the macula. *Prog Retin Eye Res.* 2013;32:1–21.
  28. Vianna JR, Malik R, Danthurebandara VM, et al. Beta and gamma peripapillary atrophy in myopic eyes with and without glaucoma. *Invest Ophthalmol Vis Sci.* 2016;57:3103–3111.
  29. Sung MS, Heo H, Piao H, et al. Parapapillary atrophy and changes in the optic nerve head and posterior pole in high myopia. *Sci Rep.* 2020;10(1):4607.
  30. Koh VT, Nah GK, Chang L, et al. Pathologic changes in highly myopic eyes of young males in Singapore. *Ann Acad Med Singap.* 2013;42(5):216–224.